

Nuclear activity in nearby galaxies

Mid - infrared imaging with the VLT [★]

R. Siebenmorgen¹, M. Haas², E. Pantin³, E. Krügel⁴, C. Leipski⁵, H.U. Käufel¹, P.O. Lagage³, A. Moorwood¹,
A. Smette⁶, and M. Sterzik⁶

¹ European Southern Observatory, Karl Schwarzschild Strasse 2, D-85748 Garching b. München, Germany

² Astronomisches Institut, Ruhr-Universität Bochum, Universitätsstr. 150, NA7, 44801 Bochum, Germany

³ UMR7158 CEA-CNRS-U. Paris 7, DSM/DAPNIA/Service d'Astrophysique, CEA/Saclay, 91191 Gif-sur-Yvette, France

⁴ Max-Planck-Institut für Radioastronomie, Auf dem Hügel 69, Postfach 2024, 53010 Bonn, Germany

⁵ Department of Physics, University of California, Santa Barbara, CA 93106, USA

⁶ European Southern Observatory, Casilla 19001, Santiago 19, Chile

Received 08/02/2008; accepted 19/05/2008

ABSTRACT

Aims. Dust enshrouded activity can ideally be studied by mid-infrared (MIR) observations. In order to explore the AGN versus star forming origin of the nuclear MIR emission of galaxies, observations of high spatial resolution are required. Here we report on 11.3 μm observations with VISIR at the VLT, reaching 0.35'' spatial resolution (FWHM).

Methods. During the scientific verification of VISIR we have observed a sample of 36 nearby galaxies having a variety of optically classified nuclear activity: 17 black hole driven active galactic nuclei (AGN), 10 starbursts (SBs) and 9 quiet spirals.

Results. 16/17 AGN are detected and unresolved, 5/10 SBs are detected and resolved with structured emission up to a few arcsec, while for 5/10 SB and all 9 quiet nuclei low upper limits are provided. The morphology of the resolved SB nuclei follows that seen at radio frequencies. The compactness of AGN and the extent of the SB nuclei is consistent with predictions from radiative transfer models and with MIR spectra of lower spatial resolution. We explore the nuclear MIR surface brightness as a quantitative measure. While AGN and SB cannot be distinguished with MIR data from 4m class telescopes, our data provide evidence that, up to a distance of 100 Mpc, AGN and SB can well be separated by means of MIR surface brightness when using 8m class telescopes.

Key words. Infrared: galaxies – Galaxies: nuclei – Galaxies: active – Galaxies: spiral

1. Introduction

The mid infrared (MIR) luminosity of the central region of galaxies has long been known to be a reliable indicator of activity much less affected by extinction than optical and NIR observations (Rieke & Lebofsky, 1978). The MIR emission traces thermal radiation from hot dust ($\sim 100\text{K}$) heated either by OB stars or black hole activity. For quasars the presence of a non-thermal synchrotron component is also conceivable. Based on data from the Infrared Space Observatory and the Spitzer Space Telescope, many diagnostics have been proposed to quantify which of the two activity types, starburst or AGN, is dominant. The diagnostics include the slope of the IR continuum, the strength of the PAH features, the ratio of high to low ionization lines and the silicate band (Genzel et al. 1998, Laurent et al. 2000, Sturm et al. 2002, Siebenmorgen et al. 2005, Hao et al. 2005, Sturm et al. 2006, Spoon et al. 2007). However, given the small sizes of these telescopes in space, the diagnostics may be contaminated by the contribution from the surrounding galaxy. In order to assess the origin of the nuclear MIR luminosity, high spatial resolution observations from larger ground-based telescopes are required.

In the past, numerous MIR studies have been undertaken to see how compact AGN are as compared to SBs. While obser-

vations with 4m class telescopes have been performed for large samples, the spatial resolution and sensitivity mostly limited the studies to a comparison between central (1'' - 5'') and extended MIR emission, AGN being relatively more compact than SBs (e.g. Roche et al. 1991, Maiolino et al. 1995, Gorjian et al. 2004), and only a few very nearby SBs could be resolved in more detail (e.g. Siebenmorgen et al. 2004, Galliano et al. 2005a using TIMMI2 at the ESO 3.6m telescope). With the advent of MIR facilities at 10m class telescopes a small number of nearby, mostly (ultra)-luminous infrared galaxies have been observed so far, successfully resolving some SBs (Soifer et al. 1999, 2000, 2001 with Keck/MIRLIN, Alonso-Herrero et al. 2006 with Gemini/T-ReCS, Galliano et al. 2005b, Wold et al. 2006 with VLT/VISIR).

Here we report on the science verification results from VISIR, the MIR instrument at the VLT (Lagage et al. 2004). We exploit VISIR's capabilities to study a sample of bright, nearby spirals and compare the observations with both radiative transfer models and radio-interferometric maps.

2. VISIR science verification observations

A sample of 36 targets with distance $< 100\text{Mpc}$ were selected from the catalog of spiral galaxies by Albrecht et al. (2007). This catalog is a complete FIR-selected sample with $S_{100\mu\text{m}} > 9\text{Jy}$ and includes 168 objects whose CO gas emission and submm emission is well studied. It is based on work previously carried out by Krügel et al. (1990), Chini et al. (1992) and Chini et al.

Send offprint requests to: rsiebenm@eso.org

[★] Based on ESO: 68.B-0066(A) and 60.A-9244(A)

(1995). Following the classification from optical spectroscopy as listed by Albrecht et al. (2007) our sample consists of: i) seventeen AGN, ii) ten starbursts and iii) nine sources classified as normal inactive spirals; their gas mass is comparable to that of the active galaxies in the sample. The median distances of the three sub-samples are similar and between 35 – 40 Mpc. The motivation for including the inactive spirals was to search for faint compact MIR emission from low-luminosity nuclear starbursts which so far may have escaped detection in low-resolution observations.

Imaging data through filter PAH2 ($11.25 \pm 0.6 \mu\text{m}$) were obtained under good and stable weather conditions during VISIR science verification in Oct. 2004 – Feb. 2005. During the observations the optical seeing was $\lesssim 1''$ and air mass $\lesssim 1.4$. The $0.127''$ pixel scale yields a $32'' \times 32''$ field of view, and for thermal background subtraction standard observations with on-array chopping and nodding amplitudes of $16''$ each were performed.

In cases where the target could not be identified in the real time display after 15min integration we switched to another object; otherwise typical integration times were 25min.

VISIR images sometimes exhibit stripes randomly triggered by a few high gain detector pixels. They are removed by dedicated reduction methods (Pantin et al. 2005). The relatively large number of bad pixels does not permit us to deconvolve the images, but noise filtering could be applied using a wavelet technique described by Starck & Murtagh (2002). In the final images unresolved sources show a FWHM of $0.35''$. Observations were bracketed by photometric standards which are provided by the observatory and used as PSF references. Photometry is derived from multi-aperture analysis on the final image. Achieved absolute photometric uncertainty is better than 10%. This error estimate is based on internal consistency and monitoring of the calibration observations. Haas et al. (2007) find also good consistency of VISIR $11.25 \mu\text{m}$ photometry of 16 Seyferts with other published measurements. In the VISIR observations we achieved a 3σ point source detection limit of $\sim 4 \text{ mJy}$ after 10min. integration. The differential observing technique permits us to detect smooth extended structure of more than $8''$, which is half the chopping and nodding amplitude.

The observations are summarized in Tab. 1 where targets are sorted by type, morphological and optical classification. The VISIR $11.25 \mu\text{m}$ photometry, resolved area, distance, observing date and total integration time are also given. With the exception of NGC 4418, the AGN observations are listed in a companion paper (Haas et al. 2007).

All but one AGN are detected and remain unresolved. The non-detection of NGC 5427 may be due to chopping in a structure-rich emission as discussed by Haas et al. (2007); this source is excluded from the following discussion. Five out of ten starbursts (SBs) show extended emission on scales of several arcsec. Low upper limits could be achieved for the remaining 5 galaxies classified as SBs and the 9 quiet spirals. Obviously, these galaxies do not have striking hot dust emission heated by nuclear activity. Notably, for 3 out of 5 undetected SBs there is no entry in NED indicating enhanced activity, thus they may actually be rather quiet.

3. MIR morphology of the galactic nucleus

The MIR luminosity of galactic nuclei often originates from a composite of starburst and AGN activity. Observations in the past suggest that the extent of the nuclear MIR emission may be used as an indicator to distinguish between dominance of both activity types. Radiative transfer models (e.g. Siebenmorgen et

al. 2004) yield quantitative predictions. Here we compare the VISIR observations with literature data and with model predictions. In addition, we check for resolved sources how far the MIR – radio correspondence holds.

3.1. AGN – core dominated

At $1.5''$ resolution Gorjian et al. (2004) detected 62 Seyfert galaxies in the MIR. All their detected sources show a central point source; extended structure was observed in: i) Arp 220, a well-known merger with starburst activity (e.g. Soifer et al. 1999, Spoon et al. 2004); ii) NGC 7469, a composite object with a Seyfert I nucleus and a circumnuclear starburst ring (Krabbe et al. 2001); iii) NGC 1068 where a set of clumps are located in the narrow line region and not associated with the torus (Galliano et al. 2005b); and iv) Mrk 1239 where the faint MIR extension claimed by Gorjian et al. (2004) cannot be confirmed by our short exposures. It is unresolved in VLA maps (Thean et al. 2000) and slightly extended in [O III] (Mulchaey et al. 1996). At $0.7''$ resolution with TIMMI2, Siebenmorgen et al. (2004) detected 15 Sy galaxies in the MIR. Their emission is dominated by an unresolved core and for some Seyferts (Cen A (Radomski et al. 2008), Circinus (Roche et al. 2006), NGC 1365, NGC 1386, NGC 4388, NGC 7582 (Wold et al. 2006), NGC 6240) additional faint extended structure is observed which contributes $\lesssim 20\%$ to the total MIR luminosity.

At $0.35''$ resolution with VISIR, all 36 Seyferts detected by Horst et al. (2006), Haas et al. (2007) and Horst et al. (2007) remain unresolved. This observation is consistent with predictions of radiative transfer models of the dust emission heated by an AGN. Intensity profiles of AGN dust models give a typical MIR extent of 4pc (FWHM, Fig. 22 in Siebenmorgen et al. 2004). This translates to an angular size of $0.08''$ at 10 Mpc and is below the spatial resolution of VISIR. VLTI provides this spatial resolution but has insufficient sensitivity except for a handful of bright AGN, such as NGC 1068 and Circinus which both show a small (few pc) flat central region of warm dust emission, that coincides with the positions of water maser emission for these galaxies (Jaffe et al. 2007). ESO's Extremely Large Telescope (ELT, 42m) will provide sufficient sensitivity combined with a 5 times higher spatial resolution than the VLTI.

3.2. Starburst – extended

All five VISIR detected starbursts show extended nuclear emission of a few arcsec and structures on sub-arcsec scale. Intensity profiles computed with radiative transfer models of dusty starbursts in which massive stars are distributed in a volume with $r = 500 \text{ pc}$ radius predict MIR extension of $\sim 160 \text{ pc}$ (FWHM, Fig. 22 in Siebenmorgen et al. 2004). At a distance of 100 Mpc this translates to an angular size of $0.35''$, the resolution limit of VISIR.

A major result from IRAS was the discovery of a linear correlation between global measured far IR and radio emission of normal galaxies (Helou et al. 1985). The global picture is that IR emission traces thermal emission of dust heated by star light whereas the radio is primarily non-thermal emission from supernovae. Both infrared and radio emission are powered by early type stars, albeit in different evolutionary states: before and during the main sequence phase they heat the dust and after the supernova explosion they produce copious synchrotron emission. This picture, however, cannot explain why the dispersion of this correlation is so small for entire galaxies spanning a wide

range in parameters. The physical scale below which this correlation breaks is $\lesssim 100$ pc for the Milky Way (Boulanger & Perault 1988), but could not be probed on this scale in detail for external galaxies with existing infrared space missions, e.g. ISO: Xu et al. (1992) or Spitzer: Murphy et al. (2006), because of limited spatial resolution. Giuricin et al. (1994) found that the nuclear MIR emission of spiral galaxies is correlated with the radio emission when probed on scales of $5''$.

VLA archive data exist for three of our sources for which we can compare the radio – MIR correlation by means of radio contour overlays on the VISIR images. Limitations are: i) the spatial resolution (FWHM) of the radio maps of $\sim 0.6''$ compared to VISIR of $0.35''$ and ii) the astrometric uncertainty of our VLT data ($\sim 0.3''$). In the following we discuss the five objects individually:

ESO126-G002

In the VISIR image (Fig.1) no central point source is detected. The MIR emission displays a circumnuclear ring structure quite similar to that found in NGC 7552 (Siebenmorgen et al. 2004). Striking emission clumps are seen $0.5''$ NW and a fainter one $0.8''$ SE from the center.

Mkn 708 (NGC 2966)

The VISIR image (Fig.1) displays a central point source on top of a $5'' \times 3''$ emission structure, extending West. The central core has a flux of 15 mJy, consistent with previous upper limits (Siebenmorgen et al. 2004). The extended component gives 70% of the total MIR luminosity and therefore we classify the nucleus as starburst dominated.

ESO500-G034

Optical spectra (Hill et al. 1999) classify ESO500-G034 as an intermediate object between AGN and starburst. Kewley et al. (2000) detect a compact radio core which argues for AGN rather than starburst heating of the dust. However the radio core remained unconfirmed in images by Corbett et al. (2002). The astrometric precision of our observation does not allow to locate the radio core in the VISIR image. The MIR image (Fig.2) displays a $3'' \times 4''$ nuclear extension. A dominant emission component is detected $0.5''$ to the NW from the nominal central position. It is resolved and contributes only $\lesssim 20\%$ to the luminosity observed with VISIR. A second fainter clump is seen $0.5''$ South. The beam size of the 6cm VLA map is $1.6''$ (FWHM) and cannot resolve the nuclear components. In the outer parts radio and MIR emission is correlated. As no dominant and unresolved luminosity component is detected we classify the MIR emission to be mainly starburst heated.

Mkn 617

This is a strongly interacting galaxy in a late stage of the merging process displaying star forming regions seen in H α (Dopita et al. 2002). X-ray spectroscopy suggests that Mkn 617 may harbor an obscured AGN (Risaliti et al. 2000). VLBI studies do not detect a compact radio core (Hill et al. 2001). The $11.7\mu\text{m}$ image by Miles et al. (1996) gives similar general size as the VISIR image (Fig.2) but does not resolve the detailed structure of the central $1''$ where individual clumps on top of a diffuse component are detected. The radio emission follows the MIR morphology in the outer parts but this correlation seems to break in the central sub-arcsec region. However, differences may also be related to insufficient spatial

resolution in the VLA map having a beam size of $0.6''$ (FWHM).

NGC 1482

IRAS observations indicate that NGC 1482 is a warm starburst galaxy with similar mass and size as M82. Its optical spectroscopic classification is that of a standard H II galaxy (Kewley et al. 2001). A multi-frequency radio continuum study is presented by Hota & Saikia (2005). Strickland et al. (2004) find no sign of AGN activity in H α and X-ray images. The soft X-ray reveals an outflow with super-wind morphology and strength similar to that seen in M82. The VISIR image (Fig.2) reveals a double nucleus with $3''$ core separation and is well correlated with the 6cm VLA map observed at $0.6''$ (FWHM) resolution.

4. Comparison with SEDs and MIR spectra

In this section we compare the nuclear $11.3\mu\text{m}$ flux with available MIR spectra and spectral energy distributions (SEDs) of the total galaxies. This comparison also involves radiative transfer calculations.

For the AGN we choose NGC 3783 and NGC 4418 and for the starbursts Mkn 617 and NGC 1482 because of completeness of available data¹. The AGN are shown in Fig. 3 and the starbursts in Fig. 4. Consistent with earlier results (e.g. Laurent et al. 2000, Brandl et al. 2006, Clavel et al. 2000, Weedmann et al. 2005) we find for our examples that i) PAH emission bands are strong in starbursts and weak or absent in AGN dominated galaxies and ii) silicate absorption is strong in starburst and type II AGN.

The Seyfert II NGC 4418 exhibits strong extinction along a nuclear diameter of less than 50 pc (FWHM, as estimated from the VISIR observations). Using radiative transfer models (Siebenmorgen et al. 2004), the SED can be fit by an AGN heated optically thick dust cloud of $A_V = 86$ mag. Extinction is computed from the outer radius $r_{\text{out}} = 450$ pc to the dust evaporation zone at ~ 1 pc and for simplicity a constant dust density profile is assumed. The model includes a central power-law heating source of $10^{11.8} L_{\odot}$.

The observed nuclear spectra of the starbursts are fitted by the SED model library of starburst nuclei by Siebenmorgen &

¹ Data of the Seyfert I NGC 3783 are from 2MASS, $3.6\mu\text{m}$ (Rieke 1978), MIR: VISIR $11.25\mu\text{m}$ (*this work*), Spitzer (Shi et al. 2006, IRS spectrum reprocessed here) and IRAS (Sanders et al. 2003). For the Seyfert II NGC 4418 the data are from NICMOS (Scoville et al. 2000), ISO (Spoon et al. 2001), IRAS (Sanders et al. 2003), $350\mu\text{m}$ (Benford 1999), $850\mu\text{m}$ (Dunne et al. 2000), and $1300\mu\text{m}$ (Albrecht et al. 2007). In addition, a MIR spectrum observed by us at the ESO's 3.6m with TIMMI2 between $8\text{--}13\mu\text{m}$ at spectral resolution of $\lambda/\Delta\lambda \sim 300$ and slit width of $3''$ is presented, our imaging at $10.4\mu\text{m}$ with TIMMI2 gives a 3σ upper limit of 30 mJy. Evans et al. (2003) reported a $10.3\mu\text{m}$ detection of 86 mJy using MIRLIN, but this value is also inconsistent with the available Spitzer spectrum (Spoon et al. 2007). Otherwise various photometric data and spectra agree.

For the starbursts: data of Mkn 617 are from 2MASS ($14''$ aperture), $11.7\mu\text{m}$ (Soifer et al. 2001), $11.25\mu\text{m}$ (*this work*) and Spitzer IRS (Brandl et al. 2006, reprocessed here), IRAS (Sanders et al. 2003), $160\mu\text{m}$ (Stickel et al. 2004), $350\mu\text{m}$ (Benford 1999), $450\mu\text{m}$ (Dunne et al. 2000) and $1300\mu\text{m}$ (Albrecht et al. 2007); and for NGC 1482 in the NIR from Hameed & Devereux (2005), 2MASS (Spinoglio et al. 1995), $11.25\mu\text{m}$ (*this work*), Spitzer IRS (Kennicutt et al. 2003), IRAS (Sanders et al. 2003), $350\mu\text{m}$ (Chini et al. 1995) and $1300\mu\text{m}$ (Albrecht et al. 2007).

Krügel (2007)². Both starburst models predict a visual extinction of $A_V = 18\text{mag}$, corresponding to $A_{10\mu\text{m}} \sim 1\text{mag}$, so that the dip at $10\mu\text{m}$ is due to silicate absorption and not caused by a blend of PAH emission features. The nuclear starburst emission spectrum is not representative for the total emission of the galaxy; this is most evident at long wavelengths (Fig.4); most of the FIR luminosity is due to large extended cold or even very cold dust emission (e.g. Siebenmorgen et al., 1999). On the other hand in AGN like NGC 4418 most of the emission up to $200\mu\text{m}$ arises from the central 500 pc region.

5. Nuclear MIR surface brightness

So far, we have seen that optically classified starburst nuclei are resolved with VISIR, while in AGN the unresolved core remains to dominate the MIR flux. In addition to the qualitative morphology criterion, it is desirable to quantify the effective gain reached, for instance, by VISIR when trying to distinguish between starburst and AGN. Therefore, we consider the nuclear MIR surface brightness S of our distance limited (100 Mpc) sample as shown in Fig. 5. For resolved sources without dominant unresolved core an area containing 80% of the flux is used (Tab. 1). For unresolved sources and non-detections an aperture with radius $0.35''$ is adopted, leading to lower and upper limits of S , respectively. The AGN are supplemented with 9 sources (<100 Mpc) observed with VISIR by Horst et al. (2006, 2007). The starbursts are supplemented with 4 resolved objects (Mrk1093, NGC 3256, NGC 6000 and NGC 7552) observed with ESO 3.6m/TIMM2 by Siebenmorgen et al. (2004). For comparison, also (ultra)-luminous IR galaxies observed with Keck/MIRLIN (Soifer et al. 2000) and Gemini/T-ReCS (Alonso-Herrero et al. 2006, Mason et al. 2007) are shown, albeit these sources are at larger distance. The striking results are:

- 1) At the spatial resolution of VISIR, AGN and SBs are clearly separated using the nuclear MIR surface brightness S as criterion. AGN are seen at $S \gg 10^4(L_\odot/\text{pc}^2)$ whereas most of the SB a factor 3 – 10 lower at $S \sim 10^3 L_\odot/\text{pc}^2$.
- 2) The AGN – SB separation is not possible with MIR data from 4m class telescopes, even when adopting the theoretical diffraction limit of $0.7''$ FWHM (small gray symbols, data as compiled from Tab. 3 in Haas et al. 2007). The twice larger PSF makes it harder to resolve starbursts and lowers the surface brightness of unresolved sources.
- 3) SBs populate a surface brightness range around and below that of Orion ($1.2 - 40 \times 10^3 L_\odot/\text{pc}^2$).³

² Model parameters are for Mkn 617: luminosity $L^{\text{tot}} = 10^{11.2} L_\odot$, size $R = 350\text{pc}$, extinction $A_V = 18\text{mag}$, ratio of the luminosity of OB stars with hot spots to the total luminosity $L_{\text{OB}}/L^{\text{tot}} = 0.6$, density of hot spots $n^{\text{hs}} = 10^4 \text{cm}^{-3}$; and for NGC 1482: $L^{\text{tot}} = 10^{10.2} L_\odot$, $R = 350\text{pc}$, $A_V = 18\text{mag}$, $L_{\text{OB}}/L^{\text{tot}} = 0.4$, $n^{\text{hs}} = 10^4 \text{cm}^{-3}$ and PAH abundance of 10% of C – which is a factor 5 larger than used for other elements of the SED model library. In order to fit the data below $5\mu\text{m}$, the starburst models of Mkn 617 and NGC 1482 are supplemented with an old stellar population represented by a black-body of $T = 3000\text{K}$.

³ We have analysed VISIR archive data of the Orion hot core. Images available are in the $0.075''$ pixel scale providing a $18'' \times 18''$ field ($\sim 0.002\text{pc}^2$). In this area the mean MIR surface brightness of the Orion hot core is $\sim 40800 L_\odot/\text{pc}^2$. Werner et al. (1976) found in a $5'$ far IR map a total luminosity of $1.2 \times 10^5 L_\odot$ emerging from a region of 0.4pc^2 . This converts to a MIR surface brightness $S \sim 1200 L_\odot/\text{pc}^2$ where we scaled the IR luminosity to that in the VISIR PAH2 filter applying $\log L_{11} \sim 1.06 \log(L) - 2.7$ (relation derived using template spectrum).

- 4) The AGN – SB separation is consistent with predictions from radiative transfer models of starburst galaxies (solid and dotted lines in Fig. 5).
- 5) The AGN – SB separation appears to hold also when comparing (U)-LIRGs observed with Keck/MIRLIN and Gemini/T-ReCS (data from Soifer et al. 1999, 2000, 2001, Alonso-Herrero et al. 2006, Mason et al. 2007).
- 6) Normal inactive galaxies have lower nuclear MIR surface brightness than SBs.

The high spatial resolution imaging provides a valuable diagnostic tool to determine the activity type of a galaxy nucleus. This diagnostics is limited by the diffraction of the telescope. It can be used for 8m class telescopes up to distances of $\sim 100\text{Mpc}$. Indeed, all our detected starbursts show resolved structures. On the other hand all unresolved sources with nuclear MIR surface brightness well above $S > 20000 L_\odot/\text{pc}^2$ are found in galactic nuclei with optical identified AGN signatures and we classify their MIR emission as AGN driven. For example, NGC1097, which displays in the MIR an unresolved core ($< 45\text{pc}$) and a surface brightness of $S = 10^4 L_\odot/\text{pc}^2$, is not AGN driven but heated from an unresolved star cluster (Mason et al. 2007). The VISIR derived S value of CenA is consistent with that found with Gemini (Radomski et al. 2008). Other caveats have to be mentioned for radio loud AGN where synchrotron radiation may dominate the nuclear MIR emission, e.g. M87 (Whysong & Antonucci 2004, Perlman et al. 2007) or low luminosity AGN such as LINERs not investigated here.

Acknowledgements. This research has made use of the NASA/IPAC Extragalactic Database (NED) and observations with the Spitzer Space Telescope which is operated by the Jet Propulsion Laboratory, California Institute of Technology, under contract with the National Aeronautics and Space Administration. M.H. is supported by the Nordrhein-Westfälische Akademie der Wissenschaften. We thank the anonymous referee for detailed critical suggestions.

References

- Albrecht M., Krügel E., Chini R., 2007, A&A 462, 575
 Alonso-Herrero A., Colina L., Packham C. et al. 2006, ApJ 652, L83
 Benford D.J., 1999, Thesis, California Institute of Technology
 Boulanger F., Perault M., 1988, ApJ 330, 964
 Brandl B.R., Bernard-Salas J., Spoon H.W.W., et al., 2006, ApJ 653, 1129
 Buchanan C. L., Gallimore J.F., O’Dea C. P., Baum S.A., Axon D.J., 2006, ApJ132, 401
 Chini R., Krügel E., Kreysa E., 1992, A&A 266, 177
 Chini R., Krügel E., Lemke R., Ward-Thompson D., 1995, A&A 295, 317
 Clavel J., Schulz B., Altieri B. et al. 2000, A&A, 357, 839
 Corbett E. A., Norris R. P., Heisler C. A., et al., 2002, ApJ 564, 650
 Dopita M. A., Pereira M., Kewley L.J., Capaccioni, M., 2002, ApJS 143, 47
 Dunne L., Eales S., Edmunds M., et al., 2000, MNRAS 315, 115
 Evans A.S., Becklin E.E., Scoville N.Z., et al., 2003, AJ 125, 2341
 Galliano E., Alloin D., Pantin E., Lagage P. O., Marco O., 2005a, A&A 438, 803
 Galliano E., Alloin D., Pantin E., Lagage P. O., 2005b, MNRAS 363, L1
 Genzel R., et al., 1998, ApJ 498, 579
 Gorjian V., Werner M.W., Jarrett T.H., 2004, ApJ 605, 156
 Giuricin G., Tamburini L., Mardirossian F., Mezzetti F., Monaco P., 1994, ApJ 427, 202
 Hameed S., Devereux N., 2005, AJ 129, 2597
 Hao L., et al., 2005, ApJ 625, L75
 Haas M., Siebenmorgen R., Pantin E., et al., 2007, A&A 473, 369
 Helou G., Soifer B.T., Rowan-Robinson M., 1985, ApJ 298, L7
 Hill T. L., Heisler C.A., Sutherland R., Hunstead R. W., 1999, AJ 117, 111
 Hill T. L., Heisler C. A., Norris R. P., Reynolds J. E., Hunstead R. W., 2001, AJ, 121, 128
 Horst H., Smette A., Poshak G., Duschl W. J., 2006, A&A 457, 17
 Horst H., Poshak G., Smette A., Duschl W. J., 2007, A&A in print.
 Hota A., Saikia D. J., 2005, MNRAS 356, 998

Table 1. Observed sample sorted by AGN, starbursts and normal galaxies. Specified is morphological type (NED), optical classification and distance D (Albrecht et al. 2007). VISIR parameters are: observing date, integration time, t_{int} , and integrated flux or 3σ upper limit in filter PAH2, $F_{11.25\mu\text{m}}$, and for resolved sources the area, A , of the MIR emission, respectively.

Name	type	activity	D (Mpc)	date	t_{int} (s)	$F_{11.25\mu\text{m}}$ (mJy)	A (pc ²)
AGN:							
NGC 4418	SAB(s)a	Sy2	28.3	2005-01-31	906	110	
Starburst:							
ESO091–G016	Sb	?	26.7	2005-02-02	1236	< 1.6	
ESO126–G002	SB(rs)ab	HII	38.5	2005-01-29	1413	305	325
ESO163–G011	SB(s)bsp	?	37.3	2005-01-29	707	< 1.6	
ESO500–G034	SB(s)0/a	HII	48.8	2005-01-27	1766	53	380
Mkn 617	SB(s)c pec	HII	62.8	2004-10-02	1843	720	465
Mkn 708	SBc	HII	25.2	2005-01-29	1236	214	123
Mkn 708 (core)						15	
Mkn 1022	SA pec	SB	51.2	2004-10-02	2089	< 0.9	
NGC 1482	SA0+ pec	HII	25.2	2004-09-25	1186	510	471
NGC 5258	SA(s)b pec	HII,LINER	90.3	2005-02-02	707	< 2.2	
NGC 5786	SAB(s)bc	?	39.2	2005-02-03	538	< 3.3	
Normal:							
ESO061–G011	S		81.3	2005-01-29	707	< 1.3	
ESO093–G003	SAB(r)0/a		24.5	2005-02-01	883	< 1.6	
ESO317–G023	SB(rs)a		35.8	2005-02-01	707	< 1.8	
ESO493–G016	Sb-c		34.7	2005-01-31	707	< 1.6	
NGC 2706	Sbc? sp		21.3	2005-01-31	1060	< 1.3	
NGC 3318	SA(sr)b		37.2	2005-01-31	1766	< 1.0	
NGC 3366	SB(rs)bc		38.1	2005-02-01	707	< 1.8	
NGC 4746	Sb sp		23.7	2005-01-31	883	< 1.4	
NGC 4900	SB(rs)c		12.0	2005-02-02	707	< 2.2	

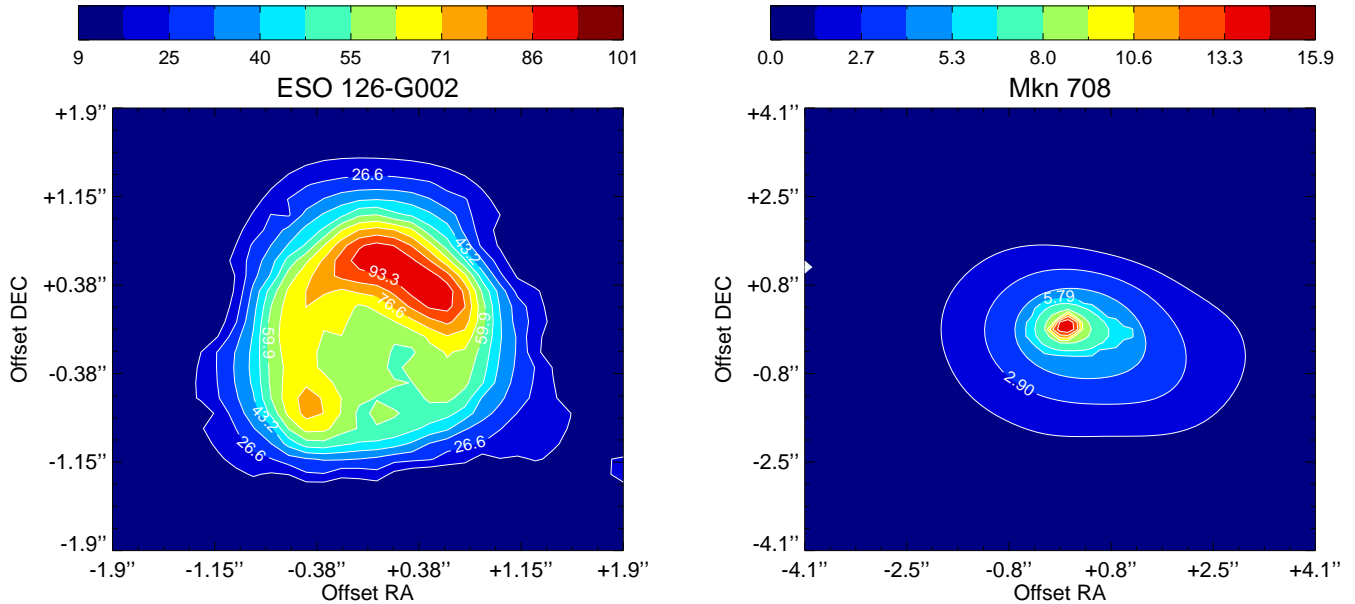


Fig. 1. VISIR image of ESO126-G002 (left) and Mkn 708 (right) in filter PAH2 (10.66 – 11.84 μm) and spatial resolution of $\sim 0.35''$ (FWHM). North is up and East is to the left. Contours and colour look-up table in mJy/arcsec².

Jaffe W., Raban D., Röttgering H., Meisenheimer K., Tristram K., 2007, in: The Central Engine of Active Galactic Nuclei, ASP Conference Series, Vol. 373, p.439
 Kennicutt R.C. Jr., Armus L., Bendo G., et al., 2003, PASP 115, 928
 Kewley L.J., Heisler C.A., Dopita M.A., et al., 2000, ApJ 530, 704
 Kewley L.J., Heisler C.A., Dopita M.A., Lumsden S., 2001, ApJS 132, 37

Krabbe A., Böker T., Maiolino R., 2001, ApJ 557, 626
 Krügel E., Chini R., Steppe H., 1990, A&A 229, 17
 Lagage P.O., Pel J., Authier M., et al., 2004, Messenger 117, 12
 Laurent O., Mirabel I. F., Charmandaris V., et al. 2000, A&A, 359, 887
 Maiolino R., Ruiz M., Rieke G.H., Keller L.D. 1995, ApJ 446, 561
 Mason R.E., Levenson N.A., Packham C., et al., 2007, ApJ 659, 249

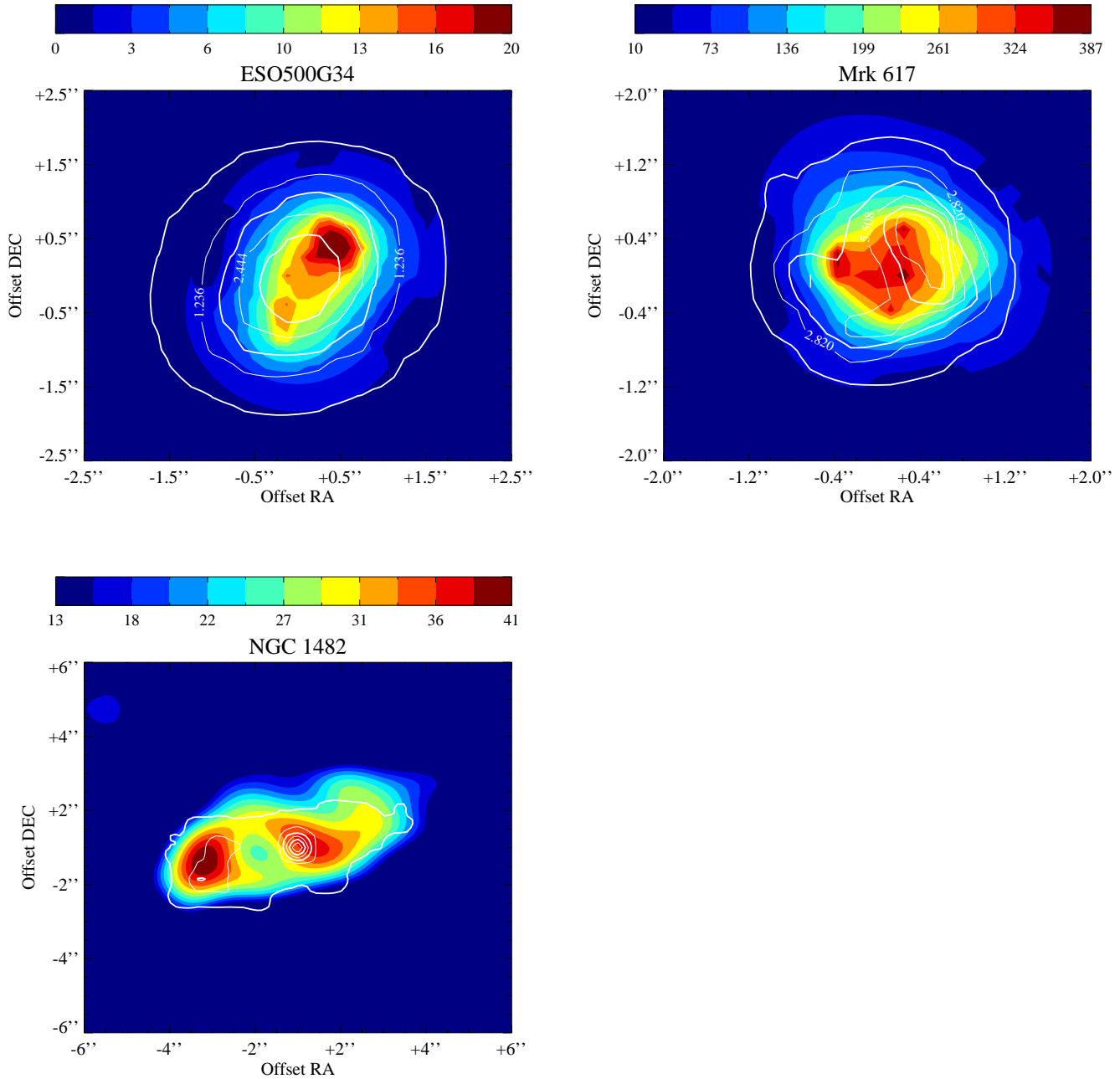


Fig. 2. VISIR images (colour look-up table in mJy/arcsec^2) overlaid with VLA 6cm radio contours. VISIR data are in filter PAH2 ($10.66 - 11.84\mu\text{m}$) at spatial resolution of $\sim 0.35''$ (FWHM). Radio contours of ESO500-G034 (beam $1.6''$, FWHM) are from 0.632 increased in steps of 0.604, that of Mkn 617 ($0.6''$) from 1.48 in steps of 1.34 and NGC 1482 ($0.6''$) from 0.618 in steps of 0.62 (mJy/arcsec^2), respectively. North is up and East is to the left.

Miles J.W., Houck J.R., Hayward T.L., Ashby M.L.N., 1996, ApJ 465, 191
 Mulchaey J.S., Wilson A.S., Tsvetanov Z., 1996, ApJS 102, 309
 Murphy E.J., Braun R., Helou G., et al., 2006, ApJ 638, 157
 Pantin E., Lagage P.-O., Claret A., et al., 2005, Messenger 119, 25
 Perلمان E., Mason R.E., Packham C., et al., 2007, ApJ 663, 808
 Rieke G.H., Lebofsky M., 1978, ApJ 220, L38
 Rieke G.H., 1978, ApJ 226, 550
 Risaliti G., Gilli R., Maiolino R., Salvati M., 2000, A&A, 357, 13
 Roche P., Aitken D., Smith C., Ward M., 1991, MNRAS 248, 606
 Roche P.F., Packham C., Telesco C.M., et al., 2006, MNRAS 367, 1689
 Radomski J.T., Packham C., Levenson N. A., et al., 2008, arXiv:0802.4119
 Sanders D.B., Mazzarella J.M., Kim D.-C., et al., 2003, AJ 126, 1607
 Scoville N. Z., Evans A. S., Thompson R., et al., 2000, AJ, 119, 991

Shi Y., Rieke G.H., Hines D.C., et al., 2006, ApJ 653, 127
 Siebenmorgen R., Krügel E., Chini, 1999, A&A 351, 495
 Siebenmorgen R., Krügel E., Spoon H. W. W., 2004, A&A 414, 123
 Siebenmorgen R., Haas M., Krügel E., Schulz B., 2005, A&A 436, L5
 Siebenmorgen R., Krügel E., 2007, A&A 461, 445
 Soifer, B. T.; Neugebauer, G.; Matthews, K., et al. 1999, ApJ 513, 207
 Soifer, B. T.; Neugebauer, G.; Matthews, K., et al. 2000, AJ, 119, 509
 Soifer, B. T.; Neugebauer, G.; Matthews, K., 2001, AJ 122, 1213
 Spinoglio L., Malkan M.A., Rush B., Carrasco L., Recillas-Cruz E., 1995, ApJ 453, 616
 Spoon H.W.W., Keane, J. V. Tielens, A.G.G.M., et al., 2001, A&A 365, L353
 Spoon H.W.W., Moorwood A.F.M., Lutz D., et al., 2004, A&A 414, 873
 Spoon H. W. W., Marshall J. A., Houck et al., 2007, ApJ 654, L49

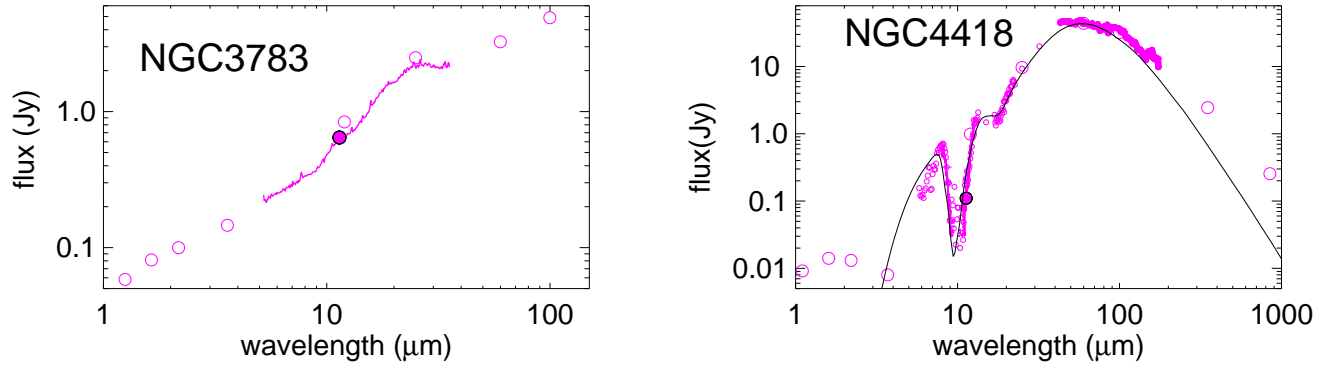


Fig. 3. SED of the Sy I galaxy NGC 3783 (*left*) and the Sy II galaxy NGC 4418 (*right*). Photometry is marked with circles and spectra with magenta lines. For both Seyferts the nuclear VISIR photometry closely resembles that of the total galaxy. This appears to hold also at FIR-mm wavelengths, as inferred from the radiative transfer model (black solid line).

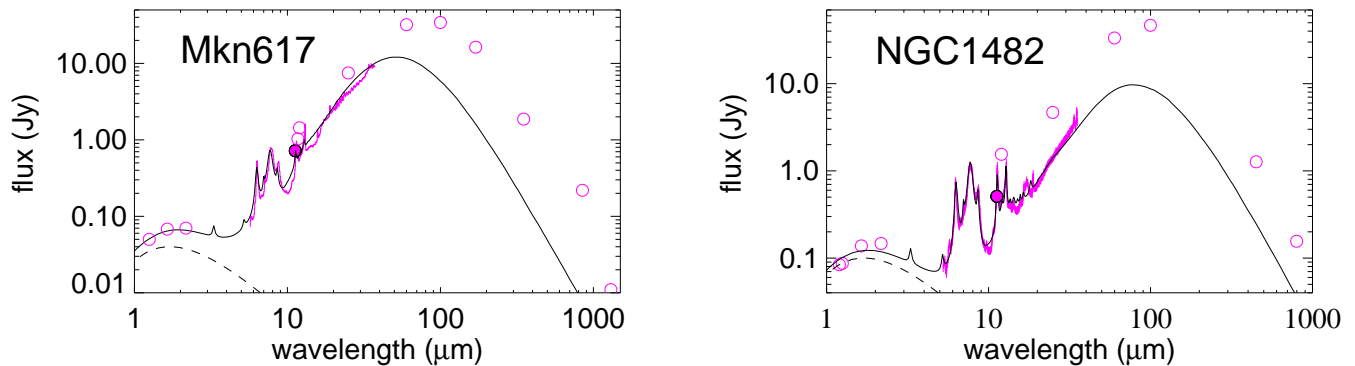


Fig. 4. SED of the starburst galaxies Mkn 617 (*left*) and NGC 1482 (*right*). Photometry is marked with circles and spectra with magenta lines. While for Mkn 617 the nuclear VISIR photometry closely resembles that of the total galaxy, the nucleus of NGC 1482 contains at most 25% of the total MIR flux. As inferred from the radiative transfer model (black solid line) the difference between nucleus and total galaxy remains (NGC 1482) and increases (Mkn 617) towards FIR-mm wavelengths. The visual extinction is in both starburst models 18mag so that the silicate band at $10\mu\text{m}$ is seen in absorption.

- Starck J.L., Murtagh, F., 2002, *Astronomical image and data analysis*, Berlin: Springer, 2002, ISBN 3540428852
- Stickel M., Lemke D., Klaas U., et al., 2004, *A&A* 422, 39
- Strickland D.K., Heckman T.M., Colbert E.J.M., Hoopes C.G., Weaver K.A., 2004, *ApJS* 151, 193
- Sturm E., Rupke D., Contursi A., et al., 2006, *ApJ*, 653, L13
- Sturm E., Lutz D., Verma A., et al., 2002, *A&A*, 393, 821
- Thean A., Pedlar A., Kukula M.J., 2000, *MNRAS* 314, 573
- Weedman D. W., Hao L., Higdon S.J.U., et al., 2005, *ApJ*, 633, 706
- Werner M.W., Gatley I., Harper D.A., et al., 1976, *ApJ* 204, 420
- Wold M., Lacy M., Käufel H.U., Siebenmorgen R., 2006, *A&A* 460, 449
- Whysong D. & Antonucci R.R., 2004, *ApJ* 602, 116
- Xu C., Klein U., Meinert D., et al., 1992, *A&A* 257, 47

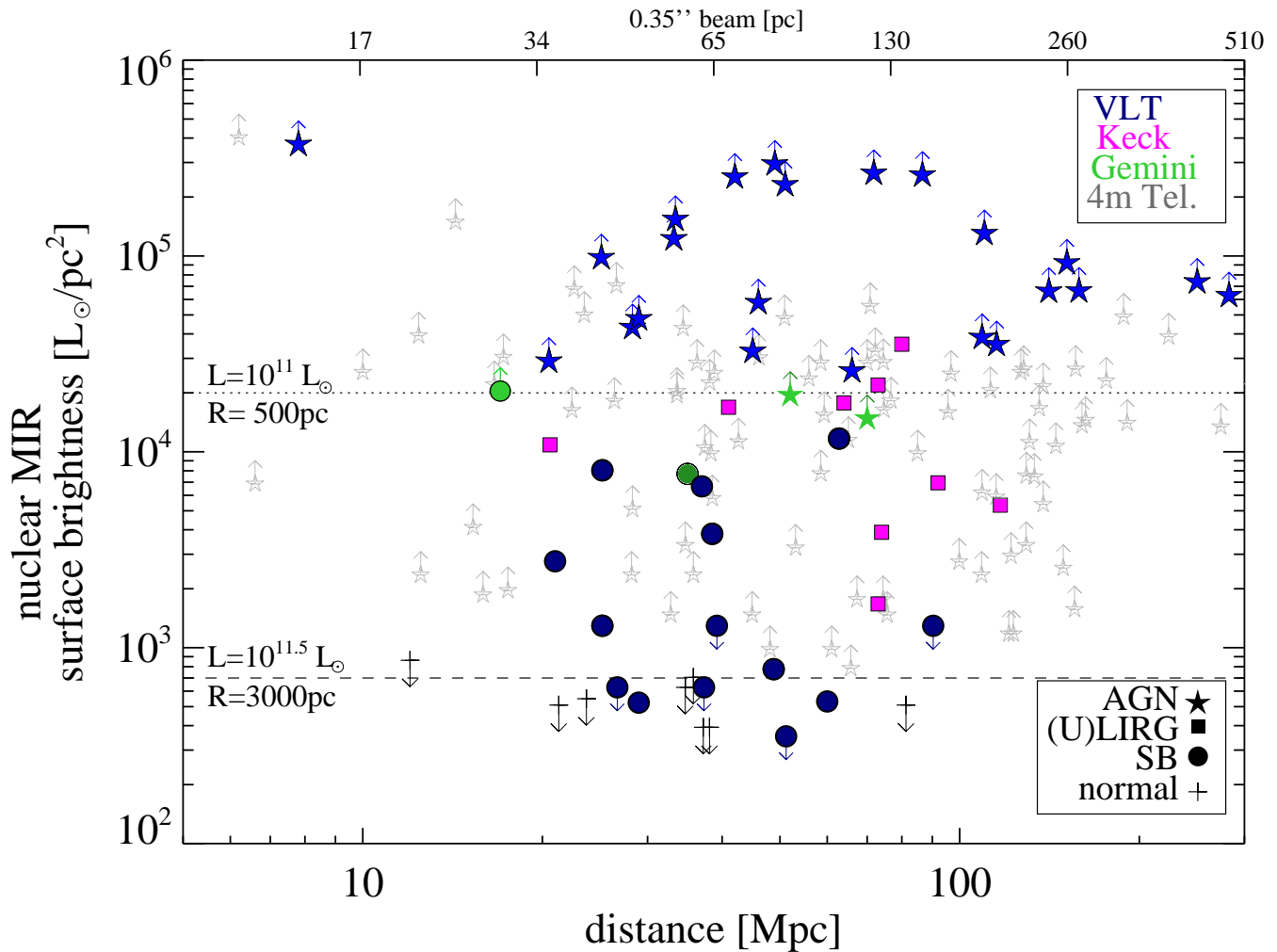


Fig. 5. Nuclear MIR surface brightness versus distance. Large symbols mark data from VLT (blue): Haas et al. (2007), Horst et al. (2006, 2007), *this work*; Keck (magenta): Soifer et al. (1999, 2000, 2001); Gemini (green): Alonso-Herrero et al. (2006), Mason et al. (2007); small symbols from 4m class telescopes (gray): Haas et al. (2007). AGN (stars) have $S > 20000 L_{\odot}/\text{pc}^2$ when observed with 8m class telescopes, starburst and (U)LIRGs are below (with the exception of VV114A which may probably harbour an AGN). Normal galaxies (+) are not detected. The horizontal dotted and long-dashed lines give the surface brightness computed with starburst models by Siebenmorgen & Krügel (2007) for given total luminosity L and where stars and dust are distributed in a $A_V = 18\text{mag}$ nucleus of radius R .